Haldane-gap excitations in the low-H_c 1-dimensional quantum antiferromagnet $Ni(C_5H_{14}N_2)_2N_3(PF_6)$ (NDMAP).

A. Zheludev,† Y. Chen,‡ C. L. Broholm,‡,♯ Z. Honda* and K. Katsumata.*
† *Physics Department, Brookhaven National Laboratory, Upton, NY 11973-5000, USA.*
‡ *Department of Physics and Astronomy, Johns Hopkins University, Baltimore, MD 21218, USA.*
♯ *NIST Center for Neutron Research, National Institute of Standards and Technology, Gaithersburg, MD 20899, USA.*
∗ *RIKEN (The Institute of Physical and Chemical Research), Wako, Saitama 351-0198, Japan.*
(February 1, 2008)

Inelastic neutron scattering on deuterated single-crystal samples is used to study Haldane-gap excitations in the new $S = 1$ one-dimensional quantum antiferromagnet $Ni(C_5H_{14}N_2)_2N_3(PF_6)$ (NDMAP), that was recently recognized as an ideal model system for high-field studies. The Haldane gap energies $\Delta_x = 0.42$ meV, $\Delta_y = 0.52$ meV and $\Delta_z = 1.86$ meV, for excitations polarized along the a, b, and c crystallographic axes, respectively, are directly measured. The dispersion perpendicular to the chain axis c is studied, and extremely weak inter-chain coupling constants $J_y = 1.8 \cdot 10^{-3}$ meV and $J_x = 3.5 \cdot 10^{-4}$ meV, along the a and b axes, respectively, are determined. The results are discussed in the context of future experiments in high magnetic fields.

75.40.Gb,75.50.Ee,75.10.Jm,73.30.Ds

I. INTRODUCTION

The unique properties of the one-dimensional (1D) integer-spin Heisenberg antiferromagnet (HAF) have captivated the minds of condensed matter physicists for the last 20 years. In total defiance of the quasi-classical picture of magnetism, the ground state in this system is a spin-singlet- a "quantum spin liquid" with only short-range (exponentially decaying) spin correlations. The excitation spectrum is also rather unique, and, even in the absense of any magnetic anisotropy, features a so-called Haldane energy gap.[1] The wealth of theoretical and experimental results accumulated to date provide a fairly complete understanding of the physics involved, and few mysteries remain, as far as the behavior of the idealized model is concerned. Particularly revealing was the neutron scattering work done on real quasi-1D $S = 1$ HAF compounds such as $CsNiCl_3$,[2] NENP $(Ni(C_2H_8N_2)_2NO_2(ClO_4))$,[3] and Y_2BaNiO_5 (Ref. 4).

One of the few remaining unresolved issues is the behavior of Haldane-gap antiferromagnets in high magnetic fields. An external magnetic field splits the triplet of Haldane excitations,[5,3,6–9] driving one of the modes to zero energy at some critical field H_c. At this soft-mode quantum phase transition, static long-range antiferromagnetic correlations appear. In essence, the external field suppresses zero-point quantum spin fluctuations that are responsible for the destruction of long-range order in the spin-liquid state, and restores long-range spin coherency. Despite the success of high-field bulk studies of several material, it has been highly frustrating, that for most existing systems the actual values of the critical fields are unobtainable in neutron scattering experiments. As a result, the properties of the high-field phase are still largely unknown. It is even unclear, whether or not the high-field phase is commensurate, and virtually nothing is known about the excitation spectrum.

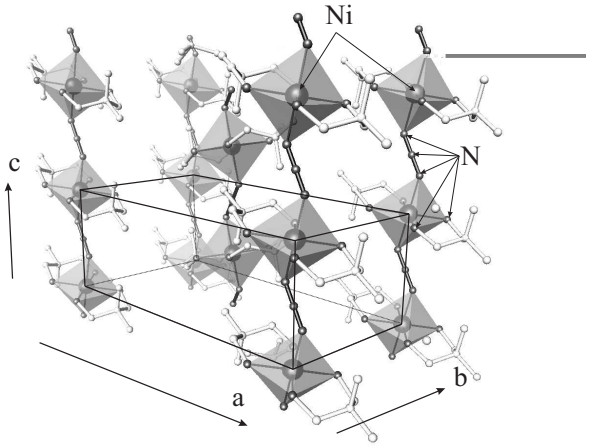

FIG. 1. A schematic view of the antiferromagnetic spin chains in the NDMAP crystal structure. Only Ni, N and C atoms are shown.

Traditionally, NENP was the workhorse of high-field studies. For this compound large single crystal samples can be fabricated, and the critical field $H_c = 9$ T (when applied parallel to the chain-axis) is, in principle, accessible in a neutron-scattering experiment. In practice, it is however easier to perform measurements with a magnetic field applied perpendicular to the spin chains. The corresponding critical field for NENP is, unfortunately, much larger: $H_c \approx 11 - 13$ T. In any case, measurements deep within the high-field phase are not possible. Moreover, due to certain structural features, the phase transition in NENP is smeared out. The g-tensors of the $S = 1$ Ni^{2+} ions are staggered in this compound and lead to an effective staggered field when an external uniform field is applied.[10–12] As a result, a static staggered magnetization appears at arbitrary weak applied fields, and,

strictly speaking, no additional spontaneous symmetry breaking occurs at H_c.

The recent discovery of NDMAP ($Ni(C_5H_{14}N_2)_2N_3(PF_6)$),[13] a relatively easily crystallized Haldane-gap compound with a critical field of only around 4 T,[14] and no staggering of g-tensors within spin chains, promises to make the high-field phase readily accessible in neutron scattering studies. The crystal structure of this material is similar to that of NENP, and is visualized in Fig. 1. The AF spin chains run along the c axis of the tetragonal structure (space group P_{nmn}, $a = 18.046$ Å, $b = 8.705$ Å, and $c = 6.139$ Å), and are composed of octahedrally-coordinated $S = 1$ Ni^{2+} ions bridged by triplets of nitrogen atoms. These long nitrogen bridges account for a realtively small in-chain AF exchange constant $J = 2.6$ meV, as estimated from bulk $\chi(T)$ measurements.[14] ESR and specific heat studies revealed a transition to the high-field phase at $H_c^{\parallel} = 3.4$ T, and $H_c^{\perp} = 5.8$ T, extrapolated to $T \to 0$, for a magnetic field applied parallel and perpendicular to the chain-axis, respectively.[14,15] This anisotropy of critical field is attributed to single-ion easy-plane magnetic anisotropy of type DS_z^2. The anisotropy constant was obtained from bulk susceptibility data: $D/J \approx 0.3$. Using the well-known numerical result $\Delta_z \approx 0.41J + 2pD$, $\Delta_x \approx 0.41J - pD$, $p \approx 2/3$,[6,16] one can thus estimate the Haldane gap energies: $\Delta_{\parallel} \approx 2.1$ meV and $\Delta_{\perp} \approx 0.54$ meV.

While NDMAP appears to be an ideal model system for neutron scattering experiments in the high-field phase, additional characterization, particularly a measurement of inter-chain interactions and in-plane anisotropy, is required before such a study can be carried out. Finding the 3D AF zone-center is especially important, since it is at this wave vector that static long-range correlations are expected to appear in the high-field phase. Obviously, inelastic neutron scattering is the most direct method to obtain this information. In the present paper we report the results of a zero-field inelastic cold-neutron scattering study of deuterated NDMAP single-crystal samples, aimed at extracting this information.

II. EXPERIMENTAL PROCEDURES AND RESULTS

Fully deuterated NDMAP single crystal samples were grown from solution as described in Ref. 13. It was observed that the crystals tend to shatter when cooled to low temperature, and even more so when warmed back up. When wrapped in aluminum foil the crystals do not fall apart, but the width of the mosaic distribution increases dramatically with thermal cycling. Most inelastic neutron scattering data were collected on a 140 mg single crystal sample that was taken trough the cooling cycle only twice. The mosaic of the as-grown sample was roughly 0.3° and increased to 1.5° and 3° after the first and second cooling, respectively. Inelastic neutron scattering measurements were performed on the SPINS 3-axis spectrometer installed on the cold neutron source at the National Institute of Standards and Technology Center for Neutron Research. Pyrolitic graphite crystals set for their (002) reflection were used as monochromator and analyzer. Beam divergences were approximately $40' - 80' - 80' - 240'$ through the instrument, with a cooled Be filter between the monochromator and sample. The measurements were done with a fixed final neutron energy $E_f = 2.8$ meV. The crystal was mounted with either the a or b crystallographic axis vertical, making $(0, k, l)$ and $(h, 0, l)$ reciprocal-space planes accessible to measurements. The sample was cooled to $T = 1.4$ K in an "ILL-Orange" cryostat with a 70 mm diameter sample well.

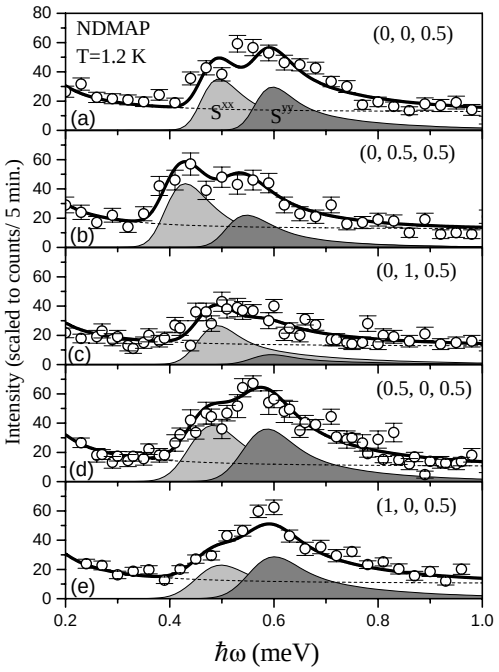

FIG. 2. Typical constant-Q scans measured at $T = 1.2$ K in an NDMAP deuterated single-crystal. Solid lines are based on global fits to the data, as described in the text. The shaded areas represent partial contributions of the a-axis and b-axis polarized Haldane gap excitations to the intensity. The dashed line indicates the background level. The magnetic excitations are resolution-limited and peak shapes are entirely defined by resolution effects.

The primary goal of the experiment was to determine the a- and b-axis dispersion relations and the polarizations of the two lower-energy Haldane-gap excitations, relevant for the soft-mode transition at H_c. Most of the data were collected in constant-Q scans at the 1D AF

zone-center $l = 0.5$ in the energy transfer range 0–1 meV. In these dispersion measurements Q-resolution is particularly important, so a flat analyzer was used. Typical scans for different momentum transfers perpendicular to the c-axis are shown in Fig. 2. At all wave vectors a well-defined peak corresponding to the lower-energy Haldane excitation doublet is clearly seen around 0.5 meV energy transfer.

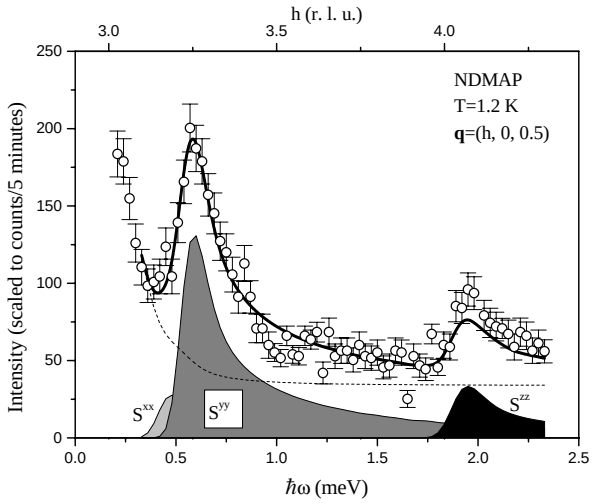

FIG. 3. A constant-$Q_{\|}$ scan measured in NDMAP using a horizontally-focusing analyzer configuration. Top axis shows the momentum transfer perpendicular to the chain-axis. Lines are as in Fig. 2.

To observe the higher-energy Haldane-gap excitation and obtain an accurate measurement of the anisotropy constant we performed a constant-Q scan in the range 0–2.4 meV (Fig. 3). To maximize intensity we used a horizontally-focusing analyzer pointing $\mathbf{c}^*$ towards the analyzer to maintain wave vector resolution along the chain. The scattering angle was varied so the projection of wave vector transfer along the chain was $0.5\mathbf{c}^*$ throughout the scan. In addition to the peak seen in the low-energy scans, a weaker feature is observed at $\hbar\omega \approx 2$ meV that can be attributed to the c-axis-polarized Haldane gap mode.

III. DATA ANALYSIS AND DISCUSSION

The measured constant-Q scans were analyzed using a parameterized model cross section, numerically convoluted with the Cooper-Nathans 3-axis spectrometer resolution function. Near the 1D AF zone-center the single mode approximation (SMA) for the dynamic structure factor of isolated Haldane spin chain is known to work extremely well.[17,18] For each channel of spin polarization the dynamic structure factor $S^{(\alpha\alpha)}(\boldsymbol{q},\omega)$ can be written as:

$$S^{(\alpha\alpha)}(\boldsymbol{q},\omega) \propto |f(q)|^2 \left(1 - \frac{\boldsymbol{q}\boldsymbol{e}_\alpha}{q^2}\right) \times$$
$$\times \frac{1-\cos(\boldsymbol{q}\boldsymbol{c})}{2} \frac{Zv}{\omega_{\alpha,\boldsymbol{q}}} \delta(\hbar\omega - \hbar\omega_{\alpha,\boldsymbol{q}}), \quad (1)$$
$$(\hbar\omega_{\alpha,\boldsymbol{q}})^2 = \Delta_\alpha^2 + v^2 \sin^2(\boldsymbol{q}\boldsymbol{c}). \quad (2)$$

Here v is the spin wave velocity, given by $v \approx 2.49J$.[19] The dimension-less constant Z defines the static staggered susceptibility of a Haldane spin chain: $\chi_\pi = Zv/\Delta$.* In the above expression we have included the magnetic form factor $f(q)$ for Ni^{2+} and the polarization factor $\left(1 - \frac{\boldsymbol{q}\boldsymbol{e}_\alpha}{q^2}\right)$. The structure factor for weakly-coupled chains can be calculated in the Random Phase Approximation (RPA).[20] The expression for $S^{(\alpha\alpha)}(\boldsymbol{q},\omega)$ does not change explicitly, but the excitations acquire dispersion perpendicular to the chain axis:

$$(\hbar\omega_{\alpha,\boldsymbol{q}})^2 = \Delta_\alpha^2 + v^2 \sin^2(\boldsymbol{q}\boldsymbol{c}) + ZvJ'(\boldsymbol{q}). \quad (3)$$

In this formula $J'(\boldsymbol{q})$ is the Fourier transform of inter-chain exchange interactions, that we assume to be isotropic (of Heisenberg type). According to numerical calculations $Z \approx 1.26$.[19] The form of J' can be guessed by looking at the crystal structure. The smallest inter-chain Ni-Ni distance (8.705Å) is along the b crystallographic axis. We shall denote the corresponding exchange constant as J_y. The next-smallest inter-chain Ni-Ni distance (10.478Å) is along the (0.5,0.5,0.5) direction. This interaction, however, is frustrated by in-chain AF interactions (any site in one chain couples to two consecutive sites in another chain), and is thus irrelevant, within the RPA, at momentum transfers $\boldsymbol{q}\boldsymbol{c} \approx \pi$. Finally, the third-smallest inter-chain distance (18.046Å) is along a. The corresponding coupling constant J_x is expected to be very small, due to the large "bond" length. The Fourier transform of inter-chain interactions can thus be written as:

$$J'(\boldsymbol{q}) = 2J_x \cos(\boldsymbol{q}\boldsymbol{a}) + 2J_y \cos(\boldsymbol{q}\boldsymbol{b}). \quad (4)$$

The chain-axis exchange constant J is not very important for our measurements: for scans collected at the 1D AF zone-center it only slightly influences the peak shapes, due to a non-zero Q-resolution along the chain-axis. We can therefore safely use the value previously obtained from susceptibility measurements. The relevant parameters of the model are thus the three gap energies Δ_x, Δ_y and Δ_z, two inter-chain exchange constants J_x and J_y and an overall intensity prefactor. Three additional parameters were used to describe the background: an energy-independent component, and the intensity and width for a Lorenzian profile centered at $\hbar\omega = 0$ to account for incompletely resolved elastic scattering.

*Here we have adopted the notation used in Ref. 21

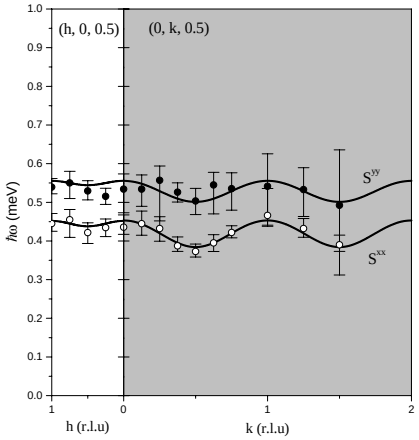

FIG. 4. Transverse dispersion of lower-energy Haldane-gap excitations in NDMAP, as determined in global fits to constant-Q scans (solid lines), as described in the text. The data points represent excitation energies obtained in fits to individual scans.

The difference between Δ_x and Δ_y, usually a result of in-plane magnetic anisotropy of type $E(S_x^2 - S_y^2)$, is too small to observe two and separate corresponding peaks in any single constant-Q scan. Distinct polarization factors for the two branches however allow us to extract both parameters in a global fit to the data measured at different momentum transfers perpendicular to the chain-axis. As a first step, we simultaneously analyzed the data collected in $(0, k, l)$ reciprocal-space plane (11 scans with a total of 382 data points). A very good global fit using Eqs. 1 and 3 is obtained with a residual $\chi^2 = 1.6$. The solid lines in Fig. 2a–c were calculated from the globally optimized parameter set. The shaded areas represent the contribution of each mode, and the dashed lines show the background level. Figure 4 (right) shows the obtained b-axis dispersion relation (solid line), that has a minimum at $k = 0.5$. Symbols in this figure represent the excitation energies obtained in fits to individual scans. A similar global fit (4 scans, 149 data points, $\chi^2 = 1.7$) was applied to all constant-Q scans measured in the $(h, 0, l)$ scattering plane (solid lines in Fig. 2d and e). In this case the excitation energies at the zone-boundary $(0, 0, 0.5)$ were fixed to the values obtained from the $(0, k, l)$-plane global fit. Only the a-axis exchange constant J_x was refined. Dispersion of magnetic excitations along this direction is barely detectable. The dispersion relation obtained from our fits is nontheless plotted in a solid line in Fig. 4 (left). The fitting analysis suggests a shallow minimum at $h = 0.5$. From Eq. 4 we can thus guess that the global minimum of the 3D dispersion (3D AF zone-center) is located at $(0.5, 0.5, 0.5)$. The energy gap for c-axis polarized excitations was determined by fitting the model cross section to the wide-range constant-Q scan measured with the horizontally-focusing configuration (Fig. 3, solid line). In this procedure the values of Δ_x and Δ_y were fixed. The parameters determined by the analysis described above are as follows: $\Delta_x = 0.42(0.03)$ meV, $\Delta_y = 0.52(0.06)$ meV, $\Delta_z = 1.86(0.1)$ meV, $J_y = 1.8(0.4) \cdot 10^{-3}$ meV, and $J_x = 3.5(3.0) \cdot 10^{-4}$ meV.

The in-chain exchange constant J and anisotropy parameter D are readily obtained from the measured gap energies:[6,16] $J \approx 0.81(\Delta_x + \Delta_y + \Delta_z) = 2.28$ meV, $D \approx \frac{1}{4}(2\Delta_z - \Delta_x - \Delta_y) = 0.70$ meV, and $D/J = 0.30$, which is consistent with the bulk susceptibility result of Ref. 14 The relative strength of inter-chain interactions are $J_y/J \approx 7 \cdot 10^{-4}$ and $J_x/J \approx 1.3 \cdot 10^{-4}$. These ratios are very similar to those found in NENP.[3]

IV. SUMMARY

The small value of critical fields in NDMAP, compared to those in NENP, are a result of smaller in-chain exchange interactions and somewhat larger easy-plane magnetic anisotropy. The lowest-energy excitation in NDMAP is polarized along the crystallograhic a–axis. The 3D magnetic zone-center appears to be $(0.5, 0.5, 0.5)$. Future experimental studies of the high-field phase should thus concentrate on this region of reciprocal space.

ACKNOWLEDGMENTS

We would like to thank S. M. Shapiro for illuminating discussions, S.-H. Lee for his assistance with the measurements at NIST, and R. Rothe for technical support at BNL. Work at Brookhaven National Laboratory was carried out under Contract No. DE-AC02-98CH10886, Division of Material Science, U.S. Department of Energy. Work at JHU was supported by the NSF through DMR-9801742. This work used instrumentation supported by NIST and the NSF through DMR-9423101. Work at RIKEN was supported in part by a Grant-in-Aid for Scientific Research from the Japanese Ministry of Education, Science, Sports and Culture.

[1] F. D. M. Haldane, Phys. Lett. **93A**, 464 (1983); Phys. Rev. Lett. **50**, 1153(1983).

[2] For a comprehensive list of references, see, for example, M. Enderle *et al.*, Europhys. Lett. **25**, 717 (1994); I. A. Zaliznyak, L.-P. Regnault and D. Petitgrand, Phys. Rev. B **50**, 15824 (1994).

[3] See reference list in L. P. Regnault, I. Zaliznyak, J. P. Renard and C. Vettier, Phys. Rev. B **50**, 9174 (1994).

[4] J. Darriet and L. P. Regnault, Solid State Commun., **86**, 409 (1993); J. F. DiTusa *et al.*, Physica B **194-196**, 181 (1994); T. Yokoo, T. Sakaguchi, K. Kakurai and J. Akimitsu, J. Phys. Soc. Japan **64**, 3651, (1995); G. Xu *et al.*, Phys. Rev. B **54**, R6827 (1996).
[5] L. P. Regnault, C. Vettier, J. Rossat-Mignod, and J. P. Renard, Physica B **180-181**, 188 (1992).
[6] O. Golinelli, T. Jolicoeur, and R. Lacaze, J. Phys. Condens. Matter **5**, 7847 (1993).
[7] K. Katsumata *et al.*, Phys. Rev. Lett. **63**, 86 (1989).
[8] I. Affleck, Phys. Rev. B **41**, 6697 (1990).
[9] T. Sakai and M. Takahashi, J. Phys. Soc. Jpn. **62**, 750 (1993).
[10] M. Chiba *et al.*, Phys. Rev. B **44**, 2838 (1991).
[11] P. P. Mitra and B. I. Halperin, Phys. Rev. Lett. **72**, 912 (1994).
[12] T. Sakai and H. Shiba, J. Phys. Soc. Jpn **63**, 867 (1994).
[13] M. Monfort, J. Ribas, X. Solans, and M. Font-Bardia, Inorg. Chem. **35**, 7633 (1996).
[14] Z. Honda, H. Asakawa, and K. Katsumata, Phys. Rev. Lett. **81**, 2566 (1998).
[15] Z. Honda, K. Katsumata, M. Hagiwara, and M. Tokunaga, Phys. Rev. B **60**, 9272 (1999).
[16] S. V. Meshkov, Phys. Rev. B **48**, 6167 (1993).
[17] S. Ma *et al.*, Phys. Rev. Lett. **69**, 3571 (1992).
[18] G. Xu *et al.*, Phys. Rev. B **54**, R6827 (1996).
[19] E. S. Sorensen and I Affleck, Phys. Rev. B**49**, 15771 (1994).
[20] R. M. Morra, W. J. L. Buyers, R. L. Armstrong, and K. Hirakawa, Phys. Rev. B **38**, 543 (1988).
[21] S. Maslov and A. Zheludev, Phys. Rev. Lett. **80**, 5786 (1998).